Biochemical Journal Immediate Publication. Published on 28 Mar 2014 as manuscript BJ20131361

Title: Acute nutrient regulation of mitochondrial glutathione redox state in pancreatic β-cells

Authors: Hilton K. Takahashi [1], Laila R. B. Santos [1], Letícia P. Roma [1], Jessica Duprez [1], Christophe Broca [2], Anne Wojtusciszyn [2] and Jean-Christophe Jonas [1]

Affiliation: [1] Université catholique de Louvain, Institut de recherche expérimentale et clinique, Pôle d'endocrinologie, diabète et nutrition, Brussels, Belgium; [2] Laboratory for Diabetes Cell Therapy, Institute for Research in Biotherapy, University Hospital St-Eloi, Montpellier 34295, France

Running title: Nutrient regulation of β-cell mitochondrial E_{GSH}

Corresponding author: Jean-Christophe Jonas, Université catholique de Louvain, Institut de recherche expérimentale et clinique, Pôle d'endocrinologie, diabète et nutrition, Avenue Hippocrate 55, UCL/IREC/EDIN B1.55.06, B-1200 Brussels, Belgium; Tel: +(32)27649575; E-mail: jean-christophe.jonas@uclouvain.be

Keywords: glucose metabolism, glutaredoxin, insulin secretion, mito-catalase, mitochondrial metabolism, NAD(P)H, rat islets, human islets, redox-sensitive GFP, SOD2

Abbreviations: Dz, diazoxide; Gn, n mM glucose; K30, 30 mM extracellular K^+; roGFP, redox sensitive Green Fluorescent Protein

Summary statement: Nutrient stimulation acutely reduces mitochondrial but not cytosolic/nuclear glutathione redox potential (E_{GSH}) in insulin-secreting β-cells under control conditions. These changes are negatively correlated with NAD(P)H autofluorescence but independent from changes in intracellular Ca^{2+} or mitochondrial pH.

THIS IS NOT THE VERSION OF RECORD - see doi:10.1042/BJ20131361

Accepted Manuscript

Licenced copy. Copying is not permitted, except with prior permission and as allowed by law.
© 2014 The Authors Journal compilation © 2014 Biochemical Society

Biochemical Journal Immediate Publication. Published on 28 Mar 2014 as manuscript BJ20131361

ABSTRACT

The glucose stimulation of insulin secretion by pancreatic β-cells depends on increased production of metabolic coupling factors, among which changes in NADPH and reactive oxygen species (ROS) may alter the glutathione redox state (E_{GSH}) and signal through changes in thiol oxidation. However, whether nutrients affect E_{GSH} in β-cell subcellular compartments is unknown. Using redox-sensitive GFP2 fused to glutaredoxin 1 and its mitochondria-targeted form, we studied the acute nutrient regulation of E_{GSH} in the cytosol/nucleus or the mitochondrial matrix of rat islet cells. These probes were mainly expressed in β-cells and reacted to low concentrations of exogenous H_2O_2 and menadione. Under control conditions, cytosolic/nuclear E_{GSH} was close to -300 mV and unaffected by glucose (from 0 to 30 mM). In comparison, mitochondrial E_{GSH} was less negative and rapidly regulated by glucose and other nutrients, ranging from -280 mV in the absence of glucose to -299 mV in 30 mM glucose. These changes were largely independent from changes in intracellular Ca^{2+} concentration and in mitochondrial pH. They were unaffected by overexpression of SOD2 and mitochondria-targeted catalase, but were inversely correlated with changes in NAD(P)H autofluorescence, suggesting that they indirectly resulted from increased NADPH availability rather than from changes in ROS concentration. Interestingly, the opposite regulation of mitochondrial E_{GSH} and NAD(P)H autofluorescence by glucose was also observed in human islets isolated from two donors. In conclusion, this study demonstrates that glucose and other nutrients acutely reduce mitochondrial but not cytosolic/nuclear E_{GSH} in pancreatic β-cells under control conditions.

INTRODUCTION

Insulin secretion by endocrine pancreatic β-cells is essential to blood glucose homeostasis. Its stimulation by glucose and other nutrients results from the acceleration of their metabolism through glycolysis and the mitochondrial Krebs cycle, with increased production of various metabolic coupling factors [1;2]. Among them, a rise in cytosolic ATP/ADP ratio leads to the closure of ATP-sensitive K^+-channels (K_{ATP} channels), plasma membrane depolarization, stimulation of Ca^{2+} influx through voltage-dependent Ca^{2+} channels, and exocytosis of insulin-containing granules. In addition to this so-called triggering pathway of glucose-stimulated insulin secretion (GSIS), a metabolic amplifying pathway of GSIS also operates, by which nutrient metabolism increases the amplitude of insulin secretion triggered by a fixed elevation of intracellular Ca^{2+} concentration [3]. Although the mechanisms of metabolic amplification of GSIS remain elusive, several metabolic coupling factors could contribute to this pathway and also modulate the triggering pathway of GSIS. They include cyclic AMP, ATP and GTP, NADPH, Krebs cycle intermediates, and long-chain acyl-CoAs (reviewed in [4;5]). A coupling role for low reactive oxygen species (ROS) concentrations in GSIS was also proposed [6-8] but remains highly controversial [9-13].

The high vulnerability of pancreatic β-cells to oxidative stress is usually ascribed to their low level of expression of hydrogen peroxide (H_2O_2)-detoxifying enzymes, such as catalase and glutathione peroxidase, in face of detectable expression of superoxide dismutase 2 (SOD2) and NADPH oxidase [12;14;15]. However, β-cells are equipped with several enzymes of the thioredoxin and glutathione redox couple systems, including the rate-limiting enzyme for glutathione synthesis γ-glutamyl-cysteine synthase, glutathione reductase, and various isoforms of glutaredoxins (GRX), thioredoxin, thioredoxin reductases and peroxiredoxins [16-18]. The

THIS IS NOT THE VERSION OF RECORD - see doi:10.1042/BJ20131361

Accepted Manuscript

Licenced copy. Copying is not permitted, except with prior permission and as allowed by law.
© 2014 The Authors Journal compilation © 2014 Biochemical Society

Biochemical Journal Immediate Publication. Published on 28 Mar 2014 as manuscript BJ20131361

glutathione oxidation ratio (or glutathione redox potential E_{GSH}) should thus be a good indicator of the balance between protein thiol oxidation, e.g. by ROS, reactive nitrogen species and other electrophiles, and the ability of β-cells to reduce them with GSH using NADPH as an electron donor to reduce oxidized glutathione (GSSG) back to GSH [19].

Recently, metabolomics analysis of β-cells stimulated with glucose for less than 15 min with or without inhibition of the pentose-phosphate pathway indicated that a positive correlation exists between GSIS and the levels of NADPH, ribose-5-phosphate and reduced glutathione (GSH) [20]. These results reinforced the hypothesis that cytosolic NADPH and GSH may be coupling factors in GSIS, e.g. through GRX1-mediated changes in the redox state of reactive thiols in cytosolic proteins [21;22]. They are also compatible with the observation that endogenous production of ROS, which are expected to trigger glutathione oxidation and NADPH consumption, negatively correlates with GSIS and long-term β-cell survival [9-12]. However, the GSH/GSSG redox couple is differently regulated in the cytosol and the mitochondrial matrix of eukaryotic cells [23], making the interpretation of changes in GSH/GSSG in total cellular extracts difficult.

Using the redox-sensitive fluorescent probe roGFP1 targeted to the mitochondrial matrix (mt-roGFP1) as an indicator of mitochondrial glutathione redox state [24], we previously showed that physiological glucose stimulation reduces mitochondrial thiol oxidation in clusters of rat pancreatic islet cells [25]. However, the changes in mt-roGFP1 fluorescence ratio, which depend on the availability of endogenous GRX, were too slow to reach steady-state within 30 min of stimulation. We have now used the redox-sensitive fluorescent probe roGFP2 fused with GRX1 to study the acute nutrient regulation of glutathione redox potential (E_{GSH}) in the cytosol/nucleus and the mitochondrial matrix of rat β-cells and confirmed the main observation in human islets from two donors [26;27].

EXPERIMENTAL

Chemicals - All chemicals were from Sigma (St-Louis, MI, USA). Restriction enzymes were from Thermo Scientific (St.Leon-Rot, Germany).

Adenoviruses - The generation of an adenovirus encoding the fluorescent protein DsRed under the control of the rat insulin promoter (RIP-DsRed) was described previously [28]. Adenoviruses encoding either GRX1-roGFP2 or mitochondrial mt-GRX1-roGFP2 under the control of the CMV promoter were generated and amplified using the AdEasy XL Adenoviral Vector System (Stratagene, La Jolla, CA, USA). Briefly, the cDNA encoding GRX1-roGFP2 and mt-GRX1-roGFP2 (a gift from Tobias Dick, German Cancer Research Center, Heidelberg, Germany) were inserted into the pShuttle-CMV vector and recloned in the adenoviral backbone plasmid pAdEasy. The resultant pAd-GRX1-roGFP2 and pAd-mt-GRX1-roGFP2 plasmids were digested with PacI and transfected into HEK-293 cells (human embryonic kidney cells) to generate adenovirus particles. After purification on a CsCl gradient, viral particles were quantified using the Adeno-X Rapid Titer Kit (Clontech, Mountain View, CA, USA). Adenoviruses coding mitochondrial catalase or SOD2 under the control of the CMV promoter were obtained from Beverly L. Davidson and John Engelhardt (University of Iowa, Gene Transfer Vector Core, Iowa

THIS IS NOT THE VERSION OF RECORD - see doi:10.1042/BJ20131361

Accepted Manuscript

Licenced copy. Copying is not permitted, except with prior permission and as allowed by law.
© 2014 The Authors Journal compilation © 2014 Biochemical Society

Biochemical Journal Immediate Publication. Published on 28 Mar 2014 as manuscript BJ20131361

City, IA, USA). The empty adenovirus (Ad-null) was kindly provided by Mark Van de Casteele (V.U.B., Brussels, Belgium).

Rat islet cell clusters - All animal experimentations were approved by the local Institutional Committee on Animal Experimentation of the Faculty of Medicine of the Université catholique de Louvain (Projects UCL/MD/2009/009 and 2013/UCL/MD/016). Islets were isolated by collagenase (Roche) digestion of the pancreas of male Wistar rats (180–200 g) as previously described [29]. They were washed and hand-picked under a stereomicroscope to ensure high purity of the preparation, then dispersed into small cell clusters using trypsin and gentle pipetting in a Ca^{2+}-free medium. These clusters were plated on glass coverslips and cultured at 37°C in the presence of 5% CO_2 with RPMI 1640 medium (Invitrogen) containing 10 mM glucose (G10), 10% FBS, penicillin and streptomycin.

Human islets - Human islets were isolated from brain-dead non-diabetic donors at the Laboratory for Diabetes Cell Therapy (Montpellier, France) according to a modified version of the automated method [30;31]. Experiments were performed in agreement with the Institutional Ethical Committee of the French Agence de la Biomédecine (ref. PFS13-008). After isolation, islets were cultured for recovery during 1-5 days in CMRL-1066 medium (InVitrogen) containing 5.6 mM glucose, 10% FBS, antibiotics and 2 mM glutamine. After shipment to Brussels, islets were cultured at 37°C in the presence of 5% CO_2 in RPMI 1640 medium containing 5 mM glucose (G5), 10% FBS, 2 mM glutamine, penicillin and streptomycin.

HEK-293 cell culture - Human embryonic kidney (HEK)-293 cells were grown in DMEM (Invitrogen) supplemented with 10% FBS, penicillin and streptomycin, and cultured at 37°C in the presence of 5% CO_2. Before adenovirus infection, the cells were trypsinized, plated on glass coverslips and cultured until they reached 70% confluence.

Adenoviral infection - Cells and islets were infected with RIP-DsRed, GRX1-roGFP2 or mt-GRX1-roGFP2 encoding adenovirus (multiplicity of infection ~50) and further cultured for 2 days before fluorescence measurements.

Confocal microscopy – The fluorescence of islet cell clusters expressing DsRed or (mt-)GRX1-roGFP2 and labelled with the nuclear stain Hoechst 33342 or the mitochondrial stain Mitotracker Red CMXRos (Invitrogen) was analyzed at room temperature using an Nikon Eclipse TE2000-E inverted microscope equipped for epifluorescence and confocal imaging (QLC100 spinning disk, Visitech International). The following range of $\lambda_{ex}/\lambda_{em}$ (nm) were used: Hoechst 33342 (epifluorescence mode, 350-370/450-470, dichroic mirror centered at 450 nm); (mt-)GRX1-roGFP2 (confocal, 491/503-552); DsRed and Mitotracker Red (confocal, 561/625-685). To allow superposition, monochrome images were converted to green, red or blue images using Image J.

Dynamic measurements of (mt-)GRX1-roGFP2 fluorescence ratio, NAD(P)H autofluorescence and intracellular Ca^{2+} concentration - After culture, the coverslip was mounted at the bottom of a 37°C temperature-controlled chamber place on the stage of an inverted microscope. Cell clusters or human islets were perifused at a flow rate of ~1 ml/min with a bicarbonate-buffered Krebs solution containing (in mM) NaCl (120), KCl (4.8), $CaCl_2$ (2.5), $MgCl_2$ (1.2), $NaHCO_3$ (24), 1 g/l BSA (fraction V; Roche) and various glucose concentrations and test substances. This solution was continuously gassed with O_2/CO_2 (94/6) to maintain pH ~7.4. The fluorescence ratio

THIS IS NOT THE VERSION OF RECORD - see doi:10.1042/BJ20131361

Accepted Manuscript

Licenced copy. Copying is not permitted, except with prior permission and as allowed by law.
© 2014 The Authors Journal compilation © 2014 Biochemical Society

Biochemical Journal Immediate Publication. Published on 28 Mar 2014 as manuscript BJ20131361

of (mt-)GRX1-roGFP2 (λ_{ex} 400/480 nm; λ_{em} 535 nm) was measured every 30 s. The results were normalized to the fluorescence ratio measured at the end of the experiment in the presence of 10 mM DTT (set to 0%) then of 1 mM H_2O_2 or 100 µM aldrithiol (set to 100%). NAD(P)H autofluorescence (λ_{ex} 360 nm; λ_{em} 470 nm) was normalized to the initial fluorescence level measured in the presence of 0.5 mM glucose. The intracellular Ca^{2+} concentration ($[Ca^{2+}]_i$) was measured in clusters or islets loaded for 2 h with 2 µM Fura-2 LR acetoxymethylester (formerly sold as FuraPE3-AM; Teflabs, Austin, TX). Fura-2 LR fluorescence ratio (λ_{ex} 340/380 nm; λ_{em} 510 nm) was acquired every 5s as described [29]. Cell clusters were imaged through a 40x objective, whole islets through a 20x objective.

Computation of (mt-)GRX1-roGFP2 oxidation ratio (OxD) and glutathione redox potential (E_{GSH}) - The oxidation ratio of (mt-)GRX1-roGFP2 (OxD) and the glutathione redox potential (E_{GSH}) were computed from the (mt-)GRX1-roGFP2 fluorescence intensities at each wavelength of excitation and their ratio under test conditions and during final normalization procedure with DTT and H_2O_2 as described by Meyer and Dick [27], using a standard redox potential of -280 mV for roGFP2 and assuming that the total glutathione concentration was similar under these various conditions and in the different cell compartments and cell types studied.

Statistics - Results are shown as means ± SE for clusters from at least 3 different preparations, except in figure 4. In each figure, the statistical significance of differences in fluorescence ratio was assessed by one-way ANOVA (for repeated measurements when the comparison was made between selected time points in the same trace) followed by a test of Newman–Keuls. These analyses were performed using GraphPad Prism version 6.02 for Windows (GraphPad Software, La Jolla, CA, USA).

RESULTS

Characterization of (mt-)GRX1-roGFP2 expression in rat islet cell clusters – To obtain high expression of the probes in various cell types, we generated two adenoviruses coding GRX1-roGFP2 or mt-GRX1-roGFP2 under the control of the CMV promoter. To check whether the probes are expressed in β-cells, rat islet cell clusters were co-infected with Ad-mt-GRX1-roGFP2 and Ad-RIP-DsRed to identify insulin-expressing β-cells (Fig. 1A). Of 147 cells from 3 coverslips analyzed, ~84% of the cells were positive for DsRed, ~78% for GFP and ~73% for both DsRed and GFP. Interestingly, ~94% of the GFP-positive cells were DsRed-positive β-cells, whereas only ~30% of the DsRed-negative cells were GFP-positive, suggesting that the adenoviral infection or the CMV promoter was more efficient in rat pancreatic β-cells than in non-β islet cells. The results obtained with the probes therefore mostly reflect changes in β-cells within islet cell clusters. We also checked the correct targeting of the probes by confocal microscopy. As shown in figure 1B, mt-GRX1-roGFP2 fluorescence was punctated and colocalized with MitoTracker-Red fluorescent dye, in agreement with its targeting to the mitochondrial matrix. A faint fluorescent signal was also detected in cell nuclei. In comparison, the fluorescence of GRX1-roGFP2 was observed in the cytosol and nucleus of rat islet cells and did not colocalize with Mitotracker-Red (Fig. 1C).

Sensitivity of (mt-)GRX1-roGFP2 to H_2O_2 and menadione in rat islet cell clusters - To further characterize the probes in rat islet cells, we tested their sensitivity to increasing concentrations of

THIS IS NOT THE VERSION OF RECORD - see doi:10.1042/BJ20131361

Accepted Manuscript

Licenced copy. Copying is not permitted, except with prior permission and as allowed by law.
© 2014 The Authors Journal compilation © 2014 Biochemical Society

Biochemical Journal Immediate Publication. Published on 28 Mar 2014 as manuscript BJ20131361

exogenous H_2O_2 and menadione, a quinone that generates superoxide in the mitochondria more than in the cytosol through futile redox cycling by various oxidoreductases [32]. To allow comparisons between experiments, the fluorescence ratios were systematically expressed in percentage of the difference between the ratio measured in the presence of 10 mM DTT (fully reduced probe, normalized ratio set to 0%) and that measured in the presence of 1 mM H_2O_2 (fully oxidized probe, normalized ratio set to 100%) at the end of each experiment. During initial perifusion with a medium containing 10 mM glucose, the normalized fluorescence ratio of GRX1-roGFP2 was lower than that of mt-GRX1-roGFP2 (~3% *vs.* ~15%, respectively), suggesting that glutathione is more oxidized in the mitochondrial matrix than in the cytosol/nucleus. As shown in figure 2AB, H_2O_2 dose-dependently increased (mt-)GRX1-roGFP2 fluorescence ratio in both compartments, with a higher sensitivity of the probe in the cytosol/nucleus than in the mitochondria. In comparison, menadione significantly increased the fluorescence ratio of both probes at 5 µM, with a larger effect in the mitochondria than in the cytosol/nucleus (Fig. 2CD).

Glucose and other nutrients acutely reduce mt-GRX1-roGFP2 fluorescence ratio and E_{GSH} in rat islet cell clusters – We next tested the effect of acute changes in glucose concentration on NAD(P)H autofluorescence, $[Ca^{2+}]_i$ and (mt-)GRX1-roGFP2 fluorescence ratio in rat islet cell clusters. As expected, glucose concentration-dependently increased NAD(P)H autofluorescence (Fig. 3A) and induced typical changes in $[Ca^{2+}]_i$, with a reduction due to Ca^{2+} pumping in the endoplasmic reticulum at 2 and 5 mM glucose, and a marked increase due to Ca^{2+} influx at 10 and 30 mM glucose (Fig. 3B). Under these conditions, glucose did not significantly affect the fluorescence ratio of GRX1-roGFP2 (Fig. 3C) but largely affected that of mt-GRX1-roGFP2 (Fig. 3D). Thus, after initial perifusion in the presence of 10 mM glucose, omission of glucose from the medium rapidly increased mt-GRX1-roGFP2 normalized fluorescence ratio from 15±1% to 31±2%; subsequent stimulation with 2, 5, 10 and 30 mM glucose rapidly decreased mt-GRX1-roGFP2 fluorescence ratio in a concentration-dependent manner to 11±1% in G30. A similar glucose-dependent reduction in mt-GRX1-roGFP2 fluorescence ratio was observed in human islets isolated from two donors, together with the expected glucose-induced rises in NAD(P)H autofluorescence and $[Ca^{2+}]_i$ (Fig. 4).

Besides glucose, we also tested the effect of several nutrients that stimulate β-cell mitochondrial metabolism and insulin secretion. As shown in figure 3EF, addition of α-ketoisocaproate (KIC), methylsuccinate or a mix of leucine and glutamine at concentrations known to stimulate insulin secretion significantly reduced mt-GRX1-roGFP2 fluorescence ratio in the presence of 5 mM glucose. In contrast, addition of leucine alone did not significantly affect mt-GRX1-roGFP2 fluorescence ratio.

To check whether the glucose regulation of mt-GRX1-roGFP2 fluorescence was a general phenomenon or a peculiarity of rat islet cells, we also performed similar experiments in HEK-293 cells. During initial perifusion with a medium containing 10 mM glucose, the normalized mt-GRX1-roGFP2 fluorescence ratio was similar to that observed in islet cell clusters exposed to 30 mM glucose (~10%), and remained unaffected upon acute changes in glucose concentration from 10 to 2 then to 30 mM (Suppl. Fig. 1).

A low H_2O_2 concentration unmasks the glucose effects on cytosolic/nuclear GRX1-roGFP2 fluorescence ratio –The lack of detectable glucose effect on GRX1-roGFP2 fluorescence ratio

THIS IS NOT THE VERSION OF RECORD - see doi:10.1042/BJ20131361

Accepted Manuscript

Licenced copy. Copying is not permitted, except with prior permission and as allowed by law.
© 2014 The Authors Journal compilation © 2014 Biochemical Society

Biochemical Journal Immediate Publication. Published on 28 Mar 2014 as manuscript BJ20131361

could be due to the almost fully reduced state of the probe under control conditions. We therefore tested the effect of glucose in the presence of a low concentration of H_2O_2 (15 µM) that increases the normalized GRX1-roGFP2 fluorescence ratio to ~20% (Fig. 5). Under these conditions, omission of glucose followed by stimulation with 30 mM glucose significantly increased then decreased GRX1-roGFP2 fluorescence ratio in rat islet cell clusters, indicating that glucose improves the β-cell ability to reduce glutathione under mild oxidative stress.

Nutrient-induced changes in mt-GRX1-roGFP2 fluorescence ratio are largely independent from changes in mitochondrial pH and Ca^{2+} influx - The mitochondrial matrix of β-cells is only slightly alkaline at resting state (pH ~7.25) and is rapidly alkalinised upon nutrient stimulation to a value close to that found in most cell types (pH ~7.7) [33]. We have previously shown that, in contrast with the H_2O_2 sensor HyPer that was markedly pH-sensitive, the thiol redox probe mt-roGFP1 was only slightly affected by changes in mitochondrial pH [25]. As roGFP2 was reported to be slightly more pH-sensitive than roGFP1, we tested whether the effect of nutrients on mt-GRX1-roGFP2 fluorescence ratio could result from the mitochondrial matrix alkalinisation they produce. However, although high concentrations of NH_4Cl and sodium acetate slightly affected mt-GRX1-roGFP2 fluorescence ratio in the presence of 10 mM glucose, these effects were transient, not significant, and going in a direction that would mask rather than contribute to the glucose effects on mt-GRX1-roGFP2 fluorescence ratio (Fig. 6). These glucose effects are therefore largely independent from changes in mitochondrial pH.

We next tested the effect of changes in Ca^{2+} influx on the glucose-induced reduction of mt-GRX1-roGFP2 fluorescence ratio. Closing K_{ATP} channels with tolbutamide in the presence of 5 mM glucose triggered a rapid increase in $[Ca^{2+}]_i$ but only tended to transiently reduce mt-GRX1-roGFP2 fluorescence ratio in rat islet cell clusters (Fig. 7AB). Conversely, opening K_{ATP} channels with diazoxide in the presence of 10 mM glucose rapidly reduced $[Ca^{2+}]_i$ but did not affect mt-GRX1-roGFP2 fluorescence ratio (Fig. 7CD). The dissociation between changes in $[Ca^{2+}]_i$ and mt-GRX1-roGFP2 fluorescent ratio was also observed when islet cell clusters were depolarized with 30 mM extracellular K^+ in the continued presence of diazoxide (large sustained increase in $[Ca^{2+}]_i$ but only small non-significant reduction in mt-GRX1-roGFP2 fluorescence ratio) and when they were submitted to changes in glucose concentration under these conditions (little change in the already elevated $[Ca^{2+}]_i$, but large significant effect of glucose on mt-GRX1-roGFP2 fluorescence ratio of similar amplitude to that observed under control conditions) (Fig. 7BD). These results strongly suggest that the glucose-mediated reduction of mt-GRX1-roGFP2 fluorescence ratio is largely independent from the rise in $[Ca^{2+}]_i$ it produces.

Effects of mitochondrial catalase and superoxide dismutase 2 overexpression on mt-GRX1-roGFP2 fluorescence ratio - β-cells express low levels/activity of antioxidant enzymes such as catalase, SOD1 and glutathione peroxidase while moderately expressing mitochondrial SOD2 [14;15;34]. To test the role of changes in mitochondrial ROS production in the glucose alteration of mt-GRX1-roGFP2 fluorescence ratio, we overexpressed catalase targeted to the mitochondria (mCAT) together with SOD2 in islets cell clusters and evaluated their effect on mt-GRX1-roGFP2 fluorescence ratio. As shown in figure 7AB, the combined enzymes significantly reduced the oxidation of the probe by both H_2O_2 and menadione in the presence of 10 mM glucose, demonstrating their efficacy as mitochondrial antioxidant under these conditions. However, they did not affect the glucose regulation of mt-GRX1-roGFP2 fluorescence ratio (Fig. 8C),

THIS IS NOT THE VERSION OF RECORD - see doi:10.1042/BJ20131361

Accepted Manuscript

Licenced copy. Copying is not permitted, except with prior permission and as allowed by law.
© 2014 The Authors Journal compilation © 2014 Biochemical Society

Biochemical Journal Immediate Publication. Published on 28 Mar 2014 as manuscript BJ20131361

suggesting that these glucose effects are independent from acute changes in mitochondrial ROS concentration.

Effects of mitochondrial poisons on mt-GRX1-roGFP2 fluorescence ratio and NAD(P)H autofluorescence – Although mitochondrial poisons and uncouplers modulate superoxide production at the level of the electron transport chain, they also rapidly affect NAD(P)H concentration in the mitochondrial matrix, which may also indirectly alter mt-GRX1-roGFP2 oxidation ratio. We first tested the effect of rotenone, an inhibitor of complex I of the electron transport chain, and sodium azide, an inhibitor of complex IV, in the presence of 2 and 30 mM glucose. Both agents depolarize the mitochondrial membrane, inhibit ATP production and the glucose stimulation of insulin secretion, and increase NAD(P)H autofluorescence in rat pancreatic islets [29], but they have also been shown to reduce the oxidation of fluorescent ROS indicators by low glucose in pancreatic β-cells [9;35]. As shown in figure 9, rotenone and azide acutely reduced mt-GRX1-roGFP2 in G2 and G30 while increasing NAD(P)H autofluorescence as expected. We also tested the effect of mitochondrial uncoupling with FCCP under the same experimental conditions. FCCP also depolarizes the mitochondrial membrane and inhibit ATP production and the glucose stimulation of insulin secretion in rat pancreatic islets [36], but it should decrease rather than increase their NAD(P)H autofluorescence. In the presence of 2 mM glucose, addition of FCCP did not affect mt-GRX1-roGFP2 fluorescence ratio nor NAD(P)H autofluorescence (Fig. 10AB). In contrast, FCCP significantly increased mt-GRX1-roGFP2 fluorescence ratio in the presence of 30 mM glucose while decreasing NAD(P)H autofluorescence (Fig. 10CD).

Correlation between mt-GRX1-roGFP2 fluorescence ratio and NAD(P)H autofluorescence – Together with the lack of effect of SOD2 and mCAT overexpression on the glucose regulation of mt-GRX1-roGFP2 fluorescence ratio, the results obtained in the presence of various glucose concentrations with or without mitochondrial poisons suggested that, in rat islet cells, mt-GRX1-roGFP2 fluorescence ratio is indirectly influenced by changes in NAD(P)H availability. As shown in figure 11, there was indeed a good negative correlation between mt-GRX1-roGFP2 fluorescence ratio and NAD(P)H autofluorescence under the various experimental conditions where both parameters were tested.

DISCUSSION

This study demonstrates that glucose and other nutrients acutely regulate the glutathione redox state (E_{GSH}) in the mitochondrial matrix but not the cytosol/nucleus of rat pancreatic β-cells under control conditions. These changes, which were also observed in two preparations of human islets but not in HEK293 cells, were largely independent from changes in $[Ca^{2+}]_i$ or mitochondrial pH. They were not affected by SOD2 and mCAT overexpression, but were inversely correlated with changes in NAD(P)H autofluorescence.

GRX1-roGFP2 is a unique rapid sensor of changes in GSH/GSSG redox equilibrium [26;27]. Its oxidation ratio computed from fluorescence measurements can be used to estimate the glutathione redox potential (E_{GSH}) in the subcellular compartments where it is expressed, at least when E_{GSH} is comprised between -320 and -240 mV. Assuming that total glutathione content was similar in the cytosol/nucleus and the mitochondrial matrix [37], our data show that E_{GSH} was

THIS IS NOT THE VERSION OF RECORD - see doi:10.1042/BJ20131361

Accepted Manuscript

Licenced copy. Copying is not permitted, except with prior permission and as allowed by law.
© 2014 The Authors Journal compilation © 2014 Biochemical Society

Biochemical Journal Immediate Publication. Published on 28 Mar 2014 as manuscript BJ20131361

close to -300 mV in the cytosol/nucleus of rat β-cells under control conditions irrespective of the glucose concentration, while it was comprised between -281 mV and -299 mV in the mitochondria of rat β-cells (and between -279 and -300 mV in the mitochondria of human islets) depending on nutrient availability (Table 2). In comparison, mitochondrial E_{GSH} in HEK293 cells was close to -300 mV. Overall, these results support the idea that E_{GSH} is usually more negative (meaning that the GSH/GSSG ratio is higher) in the cytosol than in energized mitochondria [38-40].

As expected, low micromolar concentrations of exogenous H_2O_2 and menadione dose-dependently increased GRX1-roGFP2 and mt-GRX1-roGFP2 fluorescence ratio, indicating the suitability of the probes to indirectly sense changes in ROS concentration in each compartment. This conclusion was further supported by the ability of SOD2 with mCAT overexpression to significantly prevent the effect of H_2O_2 and menadione on the mitochondrial probe. In contrast, glucose stimulation of rat β-cells rapidly and reversibly decreased mt-GRX1-roGFP2 fluorescence ratio across the whole range of concentrations tested. We consider unlikely that these glucose effects resulted from an acute rise in total glutathione in the mitochondrial matrix of rat β-cells rather than from a decrease in glutathione oxidation, because mitochondria depend on the cytosol for glutathione synthesis [23] and changes in glucose did not rapidly affect the total glutathione content of rat islets (Suppl. Fig. 2). We also consider unlikely that these results occur in the nuclei where mt-GRX1-roGFP2 was faintly expressed, because they were not observed with GRX1-roGFP2 that was strongly expressed in the nuclei.

The glucose-mediated reduction in mitochondrial E_{GSH} is in good agreement with previous studies showing that glucose rapidly reduces oxidative stress in pancreatic β-cells, an effect that was attributed to reduced ROS production or increased NADPH production [9;10;25]. The lack of effect of SOD2 with mCAT overexpression on this glucose effect suggests that it did not result from a decrease in mitochondrial ROS concentration. In contrast, several arguments plead for a role of a rise in mitochondrial NADPH concentration in these glucose effects. Such increase may result from higher production or lower consumption of NADPH, e.g. following a reduction in ROS production and degradation by NADPH dependent endogenous peroxiredoxins and glutathione peroxidase. First, a decrease in mitochondrial E_{GSH} was also triggered by mitochondrial substrates that stimulate insulin secretion while bypassing glycolysis, excluding a predominant role of cytosolic NADPH produced by glucose-6-phosphate dehydrogenase (G6PD). Second, the glucose reduction of mitochondrial E_{GSH} was inversely correlated with glucose-induced changes in NAD(P)H autofluorescence, which mainly correspond to changes occurring in the mitochondrial matrix [41]. In this context, the small effect of Ca^{2+}-influx modulating agents on β-cell mitochondrial E_{GSH} is in good agreement with their small effect on β-cell NAD(P)H autofluorescence [42]. Third, the correlation between NAD(P)H autofluorescence and mitochondrial E_{GSH} was confirmed in rat β-cells exposed to mitochondrial poisons or uncoupler that affect NAD(P)H and mitochondrial ROS production in similar or opposite ways. Thus, although the effect of rotenone and azide on mitochondrial ROS production is debated [43;44], they both increased NAD(P)H autofluorescence while decreasing mitochondrial E_{GSH}. In contrast, the mitochondrial uncoupler FCCP known to reduce both ROS production and NAD(P)H autofluorescence increased rather than decreased mitochondrial E_{GSH} in rat β-cells. Although mitochondria have long been considered to produce NADH rather than NADPH, it is now clear that the latter is produced in the mitochondrial matrix through the action of several enzymes including nicotinamide nucleotide transhydrogenase (NNT), mitochondrial isocitrate

THIS IS NOT THE VERSION OF RECORD - see doi:10.1042/BJ20131361

Accepted Manuscript

Licenced copy. Copying is not permitted, except with prior permission and as allowed by law.
© 2014 The Authors Journal compilation © 2014 Biochemical Society

Biochemical Journal Immediate Publication. Published on 28 Mar 2014 as manuscript BJ20131361

deshydrogenase and malic enzyme [2], and that the pool of NADP is increased by nutrient-mediated activation of NAD-kinase [45]. Thus, although the increase in NAD(P)H autofluorescence by rotenone/azide and its decrease by FCCP likely reflect changes in mitochondrial NADH due to the blockade or acceleration of its reoxidation by the electron transport chain, it is possible that mitochondrial NADPH also rapidly increased or decreased in parallel with NADH under these conditions, thereby modulating the ability to reduce glutathione in the mitochondrial matrix. Of course, the putative regulation of mt-GRX1-roGFP2 oxidation ratio by NADPH availability can only be indirect, for the purified probe is unable to react with NADPH in a test tube [26].

In contrast with mt-GRX1-roGFP2, GRX1-roGFP2 fluorescence ratio was not significantly affected by glucose under control conditions, ranging from -298 mV in the absence of glucose to -301 mV in the presence of 30 mM glucose. By comparing the effects of glucose and of increasing concentrations of H_2O_2, we can safely conclude that glucose does not increase cytosolic/nuclear H_2O_2 concentration by 5 µM, but we cannot exclude the possibility that glucose induces local rises in H_2O_2 concentration or a global increase below the detection level of the probe. On the contrary, it is also possible that glucose reduced cytosolic/nuclear E_{GSH} in a window over which GRX1-roGFP2 would remain largely reduced, i.e. below -300 mV. In any case, the observation that glucose acutely reduced cytosolic/nuclear E_{GSH} in β-cells exposed to a low concentration of exogenous H_2O_2 indicates that glucose metabolism improves the β-cell ability to maintain cytosolic/nuclear glutathione in the reduced state under oxidative stress conditions. It should therefore be able to do so under control conditions if glutathione is not already fully reduced.

The possible role of NADPH as a metabolic coupling factor in β-cells has been proposed to depend on GRX1-mediated changes in thiol oxidation within proteins of the exocytotic machinery [21;22]. It is possible that the changes in mitochondrial E_{GSH} we observed in pancreatic β-cells significantly change the oxidation ratio of reactive thiols within mitochondrial protein through the action of endogenous mitochondrial GRX2 and thereby affect their activity, e.g. via glutathionylation. For instance, we previously showed that the oxidation ratio of mt-roGFP1, which depends on endogenous GRX for equilibration with E_{GSH}, was rapidly increased upon lowering the glucose concentration from 10 to 2 mM, and that it more slowly decreased upon subsequent stimulation with 10 mM glucose [25]. It has also been shown that several mitochondrial proteins are differently glutathionylated depending on the redox conditions, e.g. for complex I of the mitochondrial electron transport chain and UCP 2 and 3 [46-48]. In the case of UCP2, glutathionylation was decreased by glucose stimulation of MIN6 β-cells, in agreement with the decrease in E_{GSH} we observed. These changes in protein thiol oxidation ratio may contribute to GSIS but also to the long-term nutrient regulation of β-cell survival and function. As a support of the latter possibility, it has been shown that mitochondrial NADPH production is essential in preserving cellular redox homeostasis and survival in other cell types [23]. Elucidating the mechanisms by which changes in E_{GSH} or the oxidation ratio of other redox couples depending on NADPH availability may influence pancreatic β-cells will benefit from large-scale analysis of nutrient-induced changes in thiols oxidation.

In conclusion, glucose and other nutrients acutely reduce mitochondrial but not cytosolic/nuclear E_{GSH} in rat pancreatic β-cells under control conditions.

THIS IS NOT THE VERSION OF RECORD - see doi:10.1042/BJ20131361

Accepted Manuscript

Licenced copy. Copying is not permitted, except with prior permission and as allowed by law.
© 2014 The Authors Journal compilation © 2014 Biochemical Society

Biochemical Journal Immediate Publication. Published on 28 Mar 2014 as manuscript BJ20131361

ACKNOWLEDGEMENTS

We thank Patrick Gilon for helpful comments on the manuscript, and Denis Charlier for expert technical help.

FUNDING

This work was supported by the Société Francophone du Diabète-Paris, Grant 3.4521.12 from the Fonds de la Recherche Scientifique (F.R.S.)-FNRS (Belgium), and the Communauté française de Belgique/Actions de Recherches Concertées (Grant 12/17-047). J. Duprez was recipient of a fellowship from the Fonds pour la formation à la recherche dans l'industrie et dans l'agriculture (F.R.I.A., Belgium). J.C. Jonas is Research Director of the F.R.S.-FNRS.

AUTHORS CONTRIBUTION

Conceived and designed the experiments: HKT, JCJ
Performed the experiments: HKT, LRBS
Constructed the viruses: LPR, JD
Isolated human islets: CB, AW
Analyzed the data: HKT, JCJ
Wrote the paper: HKT, JCJ
Edited and approved the paper: LPR, JD, LRBS, CB, AW

THIS IS NOT THE VERSION OF RECORD - see doi:10.1042/BJ20131361

Accepted Manuscript

Licenced copy. Copying is not permitted, except with prior permission and as allowed by law.
© 2014 The Authors Journal compilation © 2014 Biochemical Society

Biochemical Journal Immediate Publication. Published on 28 Mar 2014 as manuscript BJ20131361

REFERENCES

1 MacDonald, M. J., Fahien, L. A., Brown, L. J., Hasan, N. M., Buss, J. D., and Kendrick, M. A. (2005) Perspective: emerging evidence for signaling roles of mitochondrial anaplerotic products in insulin secretion. Am. J. Physiol. Endocrinol. Metab. **288** (1), E1-15

2 Jitrapakdee, S., Wutthisathapornchai, A., Wallace, J. C., and MacDonald, M. J. (2010) Regulation of insulin secretion: role of mitochondrial signalling. Diabetologia **53** (6), 1019-1032

3 Henquin, J. C. (2009) Regulation of insulin secretion: a matter of phase control and amplitude modulation. Diabetologia **52** (5), 739-751

4 Maechler, P. (2013) Mitochondrial function and insulin secretion. Mol Cell Endocrinol **379**, 12-18

5 Prentki, M., Matschinsky, F. M., and Madiraju, S. R. (2013) Metabolic signaling in fuel-induced insulin secretion. Cell Metab. **18** (2), 162-185

6 Bindokas, V. P., Kuznetsov, A., Sreenan, S., Polonsky, K. S., Roe, M. W., and Philipson, L. H. (2003) Visualizing superoxide production in normal and diabetic rat islets of Langerhans. J. Biol. Chem. **278** (11), 9796-9801

7 Pi, J., Bai, Y., Reece, J. M., Williams, J., Liu, D., Freeman, M. L., Fahl, W. E., Shugar, D., Liu, J., Qu, W., Collins, S., and Waalkes, M. P. (2007) Molecular mechanism of human Nrf2 activation and degradation: role of sequential phosphorylation by protein kinase CK2. Free Radic. Biol. Med. **42** (12), 1797-1806

8 Leloup, C., Tourrel-Cuzin, C., Magnan, C., Karaca, M., Castel, J., Carneiro, L., Colombani, A. L., Ktorza, A., Casteilla, L., and Penicaud, L. (2009) Mitochondrial reactive oxygen species are obligatory signals for glucose-induced insulin secretion. Diabetes **58** (3), 673-681

9 Martens, G. A., Cai, Y., Hinke, S., Stange, G., Van de Casteele, M., and Pipeleers, D. (2005) Glucose suppresses superoxide generation in metabolically responsive pancreatic β cells. J. Biol. Chem. **280** (21), 20389-20396

10 Rebelato, E., Abdulkader, F., Curi, R., and Carpinelli, A. R. (2011) Control of the intracellular redox state by glucose participates in the insulin secretion mechanism. PLoS. ONE. **6** (8), e24507

11 Sarre, A., Gabrielli, J., Vial, G., Leverve, X. M., and Assimacopoulos-Jeannet, F. (2012) Reactive oxygen species are produced at low glucose and contribute to the activation of AMPK in insulin-secreting cells. Free Radic. Biol. Med. **52**, 142-150

12 Li, N., Li, B., Brun, T., Deffert-Delbouille, C., Mahiout, Z., Daali, Y., Ma, X. J., Krause, K. H., and Maechler, P. (2012) NADPH oxidase NOX2 defines a new antagonistic role for reactive oxygen species and cAMP/PKA in the regulation of insulin secretion. Diabetes **61** (11), 2842-2850

13 Lortz, S., Gurgul-Convey, E., Naujok, O., and Lenzen, S. (2013) Overexpression of the antioxidant enzyme catalase does not interfere with the glucose responsiveness of insulin-secreting INS-1E cells and rat islets. Diabetologia **56** (4), 774-782

THIS IS NOT THE VERSION OF RECORD - see doi:10.1042/BJ20131361

Accepted Manuscript

Licenced copy. Copying is not permitted, except with prior permission and as allowed by law.

© 2014 The Authors Journal compilation © 2014 Biochemical Society

Biochemical Journal Immediate Publication. Published on 28 Mar 2014 as manuscript BJ20131361

14 Grankvist, K., Marklund, S. L., and Taljedal, I. B. (1981) CuZn-superoxide dismutase, Mn-superoxide dismutase, catalase and glutathione peroxidase in pancreatic islets and other tissues in the mouse. Biochem. J. **199** (2), 393-398

15 Tiedge, M., Lortz, S., Drinkgern, J., and Lenzen, S. (1997) Relation between antioxidant enzyme gene expression and antioxidative defense status of insulin-producing cells. Diabetes **46** (11), 1733-1742

16 Laclau, M., Lu, F., and MacDonald, M. J. (2001) Enzymes in pancreatic islets that use NADP(H) as a cofactor including evidence for a plasma membrane aldehyde reductase. Mol. Cell. Biochem. **225** (1-), 151-160

17 Godoy, J. R., Funke, M., Ackermann, W., Haunhorst, P., Oesteritz, S., Capani, F., Elsasser, H. P., and Lillig, C. H. (2011) Redox atlas of the mouse. Immunohistochemical detection of glutaredoxin-, peroxiredoxin-, and thioredoxin-family proteins in various tissues of the laboratory mouse. Biochim. Biophys. Acta **1810** (1), 2-92

18 Bensellam, M., Van Lommel, L., Overbergh, L., Schuit, F. C., and Jonas, J. C. (2009) Cluster analysis of rat pancreatic islet gene mRNA levels after culture in low-, intermediate- and high-glucose concentrations. Diabetologia **52** (3), 463-476

19 Go, Y. M. and Jones, D. P. (2008) Redox compartmentalization in eukaryotic cells. Biochim. Biophys. Acta **1780** (11), 1273-1290

20 Spegel, P., Sharoyko, V. V., Goehring, I., Danielsson, A. P., Malmgren, S., Nagorny, C. L., Andersson, L. E., Koeck, T., Sharp, G. W., Straub, S. G., Wollheim, C. B., and Mulder, H. (2013) Time-resolved metabolomics analysis of beta-cells implicates the pentose phosphate pathway in the control of insulin release. Biochem. J. **450** (3), 595-605

21 Ivarsson, R., Quintens, R., Dejonghe, S., Tsukamoto, K., In, 't, V, Renstrom, E., and Schuit, F. C. (2005) Redox control of exocytosis: regulatory role of NADPH, thioredoxin, and glutaredoxin. Diabetes **54** (7), 2132-2142

22 Reinbothe, T. M., Ivarsson, R., Li, D. Q., Niazi, O., Jing, X., Zhang, E., Stenson, L., Bryborn, U., and Renstrom, E. (2009) Glutaredoxin-1 mediates NADPH-dependent stimulation of calcium-dependent insulin secretion. Mol. Endocrinol. **23** (6), 893-900

23 Mari, M., Morales, A., Colell, A., Garcia-Ruiz, C., Kaplowitz, N., and Fernandez-Checa, J. C. (2013) Mitochondrial glutathione: features, regulation and role in disease. Biochim. Biophys. Acta **1830** (5), 3317-3328

24 Meyer, A. J., Brach, T., Marty, L., Kreye, S., Rouhier, N., Jacquot, J. P., and Hell, R. (2007) Redox-sensitive GFP in Arabidopsis thaliana is a quantitative biosensor for the redox potential of the cellular glutathione redox buffer. Plant J. **52** (5), 973-986

25 Roma, L. P., Duprez, J., Takahashi, H. K., Gilon, P., Wiederkehr, A., and Jonas, J. C. (2012) Dynamic measurements of mitochondrial hydrogen peroxide concentration and glutathione redox state in rat pancreatic β-cells using ratiometric fluorescent proteins: confounding effects of pH with HyPer but not roGFP1. Biochem. J. **441**, 971-978

THIS IS NOT THE VERSION OF RECORD - see doi:10.1042/BJ20131361

Accepted Manuscript

Licenced copy. Copying is not permitted, except with prior permission and as allowed by law.
© 2014 The Authors Journal compilation © 2014 Biochemical Society

Biochemical Journal Immediate Publication. Published on 28 Mar 2014 as manuscript BJ20131361

26 Gutscher, M., Pauleau, A. L., Marty, L., Brach, T., Wabnitz, G. H., Samstag, Y., Meyer, A. J., and Dick, T. P. (2008) Real-time imaging of the intracellular glutathione redox potential. Nat. Methods **5** (6), 553-559

27 Meyer, A. J. and Dick, T. P. (2010) Fluorescent protein-based redox probes. Antioxid. Redox Signal. **13** (5), 621-650

28 Quoix, N., Cheng-Xue, R., Mattart, L., Zeinoun, Z., Guiot, Y., Beauvois, M. C., Henquin, J. C., and Gilon, P. (2009) Glucose and pharmacological modulators of ATP-sensitive K^+ channels control $[Ca^{2+}]_c$ by different mechanisms in isolated mouse α-cells. Diabetes **58** (2), 412-421

29 Khaldi, M. Z., Guiot, Y., Gilon, P., Henquin, J. C., and Jonas, J. C. (2004) Increased glucose sensitivity of both triggering and amplifying pathways of insulin secretion in rat islets cultured for one week in high glucose. Am. J. Physiol. Endocrinol. Metab. **287**, E207-E217

30 Ricordi, C., Lacy, P. E., Finke, E. H., Olack, B. J., and Scharp, D. W. (1988) Automated method for isolation of human pancreatic islets. Diabetes **37** (4), 413-420

31 Bucher, P., Mathe, Z., Morel, P., Bosco, D., Andres, A., Kurfuest, M., Friedrich, O., Raemsch-Guenther, N., Buhler, L. H., and Berney, T. (2005) Assessment of a novel two-component enzyme preparation for human islet isolation and transplantation. Transplantation **79** (1), 91-97

32 Chuang, Y. Y., Chen, Y., Gadisetti, Chandramouli, V. R., Cook, J. A., Coffin, D., Tsai, M. H., DeGraff, W., Yan, H., Zhao, S., Russo, A., Liu, E. T., and Mitchell, J. B. (2002) Gene expression after treatment with hydrogen peroxide, menadione, or t-butyl hydroperoxide in breast cancer cells. Cancer Res. **62** (21), 6246-6254

33 Wiederkehr, A., Park, K. S., Dupont, O., Demaurex, N., Pozzan, T., Cline, G. W., and Wollheim, C. B. (2009) Matrix alkalinization: a novel mitochondrial signal for sustained pancreatic β-cell activation. EMBO J. **28** (4), 417-428

34 Tonooka, N., Oseid, E., Zhou, H., Harmon, J. S., and Robertson, R. P. (2007) Glutathione peroxidase protein expression and activity in human islets isolated for transplantation. Clin. Transplant. **21** (6), 767-772

35 Sarre, A., Gabrielli, J., Vial, G., Leverve, X. M., and Assimacopoulos-Jeannet, F. (2012) Reactive oxygen species are produced at low glucose and contribute to the activation of AMPK in insulin-secreting cells. Free Radic. Biol. Med. **52**, 142-150

36 Ortsater, H., Liss, P., Akerman, K. E., and Bergsten, P. (2002) Contribution of glycolytic and mitochondrial pathways in glucose-induced changes in islet respiration and insulin secretion. Pflugers Arch. **444** (4), 506-512

37 Lash, L. H. (2005) Role of glutathione transport processes in kidney function. Toxicol. Appl. Pharmacol. **204** (3), 329-342

38 Garcia, J., Han, D., Sancheti, H., Yap, L. P., Kaplowitz, N., and Cadenas, E. (2010) Regulation of mitochondrial glutathione redox status and protein glutathionylation by respiratory substrates. J. Biol. Chem. **285** (51), 39646-39654

THIS IS NOT THE VERSION OF RECORD - see doi:10.1042/BJ20131361

Accepted Manuscript

Licenced copy. Copying is not permitted, except with prior permission and as allowed by law.

© 2014 The Authors Journal compilation © 2014 Biochemical Society

Biochemical Journal Immediate Publication. Published on 28 Mar 2014 as manuscript BJ20131361

39 Hu, J., Dong, L., and Outten, C. E. (2008) The redox environment in the mitochondrial intermembrane space is maintained separately from the cytosol and matrix. J. Biol. Chem. **283** (43), 29126-29134

40 Ostergaard, H., Tachibana, C., and Winther, J. R. (2004) Monitoring disulfide bond formation in the eukaryotic cytosol. J. Cell. Biol. **166** (3), 337-345

41 Patterson, G. H., Knobel, S. M., Arkhammar, P., Thastrup, O., and Piston, D. W. (2000) Separation of the glucose-stimulated cytoplasmic and mitochondrial NAD(P)H responses in pancreatic islet beta cells. Proc. Natl. Acad. Sci. USA **97** (10), 5203-5207

42 Gilon, P. and Henquin, J. C. (1992) Influence of membrane potential changes on cytoplasmic Ca^{2+} concentration in an electrically excitable cell, the insulin-secreting pancreatic B-cell. J. Biol. Chem. **267** (29), 20713-20720

43 Martens, G. A., Cai, Y., Hinke, S., Stange, G., Van de Casteele, M., and Pipeleers, D. (2005) Glucose suppresses superoxide generation in metabolically responsive pancreatic β cells. J. Biol. Chem. **280** (21), 20389-20396

44 Nodin, C., Zhu, C., Blomgren, K., Nilsson, M., and Blomstrand, F. (2012) Decreased oxidative stress during glycolytic inhibition enables maintenance of ATP production and astrocytic survival. Neurochem. Int. **61** (3), 291-301

45 Gray, J. P., Alavian, K. N., Jonas, E. A., and Heart, E. A. (2012) NAD kinase regulates the size of the NADPH pool and insulin secretion in pancreatic beta-cells. Am. J. Physiol. Endocrinol. Metab. **303** (2), E191-E199

46 Mailloux, R. J., Fu, A., Robson-Doucette, C., Allister, E. M., Wheeler, M. B., Screaton, R., and Harper, M. E. (2012) Glutathionylation state of uncoupling protein-2 and the control of glucose-stimulated insulin secretion. J. Biol. Chem. **287** (47), 39673-39685

47 Beer, S. M., Taylor, E. R., Brown, S. E., Dahm, C. C., Costa, N. J., Runswick, M. J., and Murphy, M. P. (2004) Glutaredoxin 2 catalyzes the reversible oxidation and glutathionylation of mitochondrial membrane thiol proteins: implications for mitochondrial redox regulation and antioxidant defense. J. Biol. Chem. **279** (46), 47939-47951

48 Mailloux, R. J., Xuan, J. Y., Beauchamp, B., Jui, L., Lou, M., and Harper, M. E. (2013) Glutaredoxin-2 is required to control proton leak through uncoupling protein-3. J. Biol. Chem. **288** (12), 8365-8379

49 Roma, L. P., Pascal, S. M., Duprez, J., and Jonas, J. C. (2012) Mitochondrial oxidative stress contributes differently to rat pancreatic islet cell apoptosis and insulin secretory defects after prolonged culture in a low non-stimulating glucose concentration. Diabetologia **55** (8), 2226-2237

THIS IS NOT THE VERSION OF RECORD - see doi:10.1042/BJ20131361

Accepted Manuscript

Licenced copy. Copying is not permitted, except with prior permission and as allowed by law.
© 2014 The Authors Journal compilation © 2014 Biochemical Society

Biochemical Journal Immediate Publication. Published on 28 Mar 2014 as manuscript BJ20131361

TABLE 1. Computed (mt-)GRX1-roGFP2 oxidation ratios (OxD) and glutathione redox potential (E_{GSH}) in rat islet cell clusters perifused under various experimental conditions tested in figure 2. [a] $P<0.05$, [b] $P<0.01$, [c] $P<0.001$ and [d] $P<0.0001$ *vs.* G10.

Probe / Cell type	Experimental condition	OxD	E_{GSH} (mV)
GRX1-roGFP2			
Rat islet cells	G10	0.19 ± 0.02	-300.5 ± 1.7
	G10 + H_2O_2 1 µM	0.18 ± 0.02	-300.9 ± 1.8
	G10 + H_2O_2 5 µM	0.22 ± 0.02	-297.9 ± 1.4
	G10 + H_2O_2 10 µM	0.27 ± 0.01 [c]	-293.5 ± 0.8
	G10 + H_2O_2 20 µM	0.42 ± 0.01 [d]	-284.2 ± 1.2 [d]
	G10	0.19 ± 0.02	-300.0 ± 1.6
	G10 + menadione 1 µM	0.18 ± 0.02	-300.9 ± 1.7
	G10 + menadione 2.5 µM	0.19 ± 0.02	-300.7 ± 1.9
	G10 + menadione 5 µM	0.30 ± 0.03 [b]	-293.2 ± 2.5 [b]
mt-GRX1-roGFP2			
Rat islet cells	G10	0.30 ± 0.02	-291.3 ± 1.0
	G10 + H_2O_2 1 µM	0.29 ± 0.02	-292.0 ± 0.9
	G10 + H_2O_2 5 µM	0.28 ± 0.02	-292.6 ± 1.1
	G10 + H_2O_2 10 µM	0.29 ± 0.02	-291.9 ± 1.2
	G10 + H_2O_2 20 µM	0.33 ± 0.04	-289.1 ± 2.2
	G10 + H_2O_2 50 µM	0.63 ± 0.11 [d]	-271.5 ± 7.0 [d]
	G10	0.28 ± 0.04	-293.3 ± 2.7
	G10 + menadione 1 µM	0.28 ± 0.05	-293.3 ± 3.2
	G10 + menadione 2.5 µM	0.33 ± 0.07	-289.0 ± 4.5
	G10 + menadione 5 µM	0.56 ± 0.16 [a]	-276.4 ± 9.2 [a]

THIS IS NOT THE VERSION OF RECORD - see doi:10.1042/BJ20131361

Accepted Manuscript

Licenced copy. Copying is not permitted, except with prior permission and as allowed by law.
© 2014 The Authors Journal compilation © 2014 Biochemical Society

Biochemical Journal Immediate Publication. Published on 28 Mar 2014 as manuscript BJ20131361

TABLE 2. Computed (mt-)GRX1-roGFP2 oxidation ratios (OxD) and glutathione redox potential (E_{GSH}) in rat islet cell clusters, human islets and HEK-293 cells perifused under various experimental conditions tested in figures 3, 4 and suppl. figure 1. [a] $P<0.05$, [b] $P<0.01$, [c] $P<0.001$ and [d] $P<0.0001$ *vs.* G10 (or *vs.* G5 for human islets); [e] $P<0.05$ and [f] $P<0.005$ for the effect of nutrients in G5.

Probe / Cell type	Experimental condition	OxD	E_{GSH} (mV)
GRX1-roGFP2			
Rat islet cells	G10	0.18 ± 0.01	-301.0 ± 1.2
	G0	0.22 ± 0.02	-297.9 ± 1.6
	G2	0.21 ± 0.01	-297.9 ± 1.0
	G5	0.19 ± 0.01	-299.2 ± 1.1
	G10	0.18 ± 0.01	-300.8 ± 1.1
	G30	0.18 ± 0.02 [d]	-301.3 ± 1.7
mt-GRX1-roGFP2			
Rat islet cells	G10	0.28 ± 0.04	-292.7 ± 2.8
	G0	0.48 ± 0.06 [d]	-281.0 ± 3.2 [d]
	G2	0.42 ± 0.06 [c]	-284.4 ± 3.2 [c]
	G5	0.36 ± 0.03 [b]	-287.6 ± 2.4 [b]
	G10	0.29 ± 0.02	-292.7 ± 1.2
	G30	0.21 ± 0.03	-298.7 ± 2.4
	G10	0.28 ± 0.02	-293.0 ± 1.7
	G5	0.36 ± 0.10	-288.8 ± 2.0
	G5+Leu	0.31 ± 0.02	-290.8 ± 1.0
	G5+Leu+Glu	0.29 ± 0.02	-291.8 ± 1.8
	G5+KIC	0.26 ± 0.02 [e]	-294.5 ± 1.8 [e]
	G5+SM	0.19 ± 0.05 [a, f]	-298.2 ± 1.2 [a, f]
Human islets	G5	0.43 ± 0.03	-284.2 ± 1.6
	G0	0.53 ± 0.03 [c]	-278.6 ± 1.5 [c]
	G2	0.50 ± 0.02 [a]	-279.8 ± 1.3 [a]
	G5	0.36 ± 0.02 [b]	-288.3 ± 1.5 [b]
	G10	0.27 ± 0.02 [b]	-294.5 ± 1.7 [b]
	G30	0.20 ± 0.03 [c]	-299.8 ± 2.0 [c]
HEK-293 cells	G10	0.16 ± 0.02	-303.6 ± 4.8
	G2	0.17 ± 0.03	-300.2 ± 5.8
	G30	0.19 ± 0.02	-298.4 ± 4.1

THIS IS NOT THE VERSION OF RECORD - see doi:10.1042/BJ20131361

Accepted Manuscript

Licenced copy. Copying is not permitted, except with prior permission and as allowed by law.
© 2014 The Authors Journal compilation © 2014 Biochemical Society

Biochemical Journal Immediate Publication. Published on 28 Mar 2014 as manuscript BJ20131361

TABLE 3. Computed mt-GRX1-roGFP2 oxidation ratios (OxD) and mitochondrial glutathione redox potential (E_{GSH}) in rat islet cell clusters perifused under various experimental conditions tested in figure 7. [a] $P<0.01$, [b] $P<0.001$ *vs.* G10.

Experimental condition	OxD	E_{GSH} (mV)
G10	0.26 ± 0.02	-294.0 ± 1.6
G10+Dz	0.25 ± 0.02	-295.2 ± 2.0
G10K30Dz	0.23 ± 0.01	-296.8 ± 1.0
G2K30Dz	0.39 ± 0.01 [b]	-286.2 ± 1.7 [b]
G30K30Dz	0.27 ± 0.03	-294.2 ± 2.0
G10	0.29 ± 0.01	-292.8 ± 0.5
G5	0.35 ± 0.01 [b]	-287.7 ± 1.1 [a]
G5+Tolb	0.38 ± 0.02 [b]	-286.7 ± 1.9 [a]

THIS IS NOT THE VERSION OF RECORD - see doi:10.1042/BJ20131361

Accepted Manuscript

Licenced copy. Copying is not permitted, except with prior permission and as allowed by law.
© 2014 The Authors Journal compilation © 2014 Biochemical Society

Biochemical Journal Immediate Publication. Published on 28 Mar 2014 as manuscript BJ20131361

FIGURE LEGENDS

FIGURE 1. Expression of (mt-)GRX1-roGFP2 probes in rat islet cell clusters. A, the proportion of β-cells and non-β-cells expressing mt-GRX1-roGFP2 was determined by co-infection with an adenovirus encoding DsRed under the control of the rat insulin promoter (RIP-DsRed). Cell nuclei were labeled with Hoechst 33342, to allow counting the proportion of cells expressing each protein. The results are representative of images acquired from 3 coverslips using a 40x objective. B, C, confocal imaging (100x objective) of rat islet cell clusters expressing mt-GRX1-roGFP2 (B, left panel) or GRX1-roGFP2 (C, left panel) and labeled with 200 nM MitoTracker-Red (B, C, middle panels). Co-localization of (mt-)GRX1-roGFP2 and Mitoctracker Red is seen as yellow dots on merged images (B, C, right panels). Scale bars = 40 µm.

FIGURE 2. Effects of H_2O_2 and menadione on (mt-)GRX1-roGFP2 fluorescence ratio. Islet cell clusters expressing mt-GRX-roGFP2 (A, C) or GRX1-roGFP2 (B, D) were perifused with a Krebs solution containing 10 mM glucose (G10) and exposed to increasing concentrations of H_2O_2 (A, B) or menadione (C, D) before final application of 10 mM DTT then 1 mM H_2O_2 in the presence of G10 for normalization of the traces. Results are means ± SE for 3 experiments. * $P<0.05$, # $P<0.01$ and § $P<0.001$ *vs.* G10. The corresponding probe oxidation ratios (OxD) and glutathione redox potentials (E_{GSH}) are shown in table 1.

FIGURE 3. Effects of glucose and other nutrients on NAD(P)H autofluorescence, $[Ca^{2+}]_i$ and (mt-)GRX1-roGFP2 fluorescence ratio in perifused islet cell clusters. A, effects of increasing glucose concentrations (Gn in mM) on NAD(P)H autofluorescence expressed as a percentage of the average fluorescence level during initial perifusion with G0.5. B, effects of glucose on fura-2 LR fluorescence ratio as an indicator of $[Ca^{2+}]_i$. C, D, effects of glucose on GRX1-roGFP2 (C) or mt-GRX1-roGFP2 (D) fluorescence ratios. Data were normalized to the ratio measured in the presence of 10 mM DTT (set to 0%) and that measured in 1 mM H_2O_2 (set to 100%). E, effect of the addition of 5 mM α-ketoisocaproic acid (KIC) to 5 mM glucose on the normalized mt-GRX1-roGFP2 fluorescence ratio. F, comparison of the effect of 5 mM leucine (Leu), 5 mM leucine + 5 mM glutamine (LeuGln), 5 mM α-ketoisocaproic acid (KIC) or 5 mM succinate methylester (SM) in G5 following the protocol shown in panel E. Results are means ± SE for 3 experiments. A, B, * $P<0.01$ and ** $P<0.001$ *vs.* G0.5 and # $P<0.001$ for the effect of azide. D, * $P<0.05$, # $P<0.01$ and § $P<0.001$ *vs.* G0. E, F, * $P<0.001$ *vs.* G10, # $P<0.05$ and § $P<0.001$ for the effect of nutrients in G5. The corresponding probe oxidation ratios (OxD) and glutathione redox potentials (E_{GSH}) are shown in table 2.

FIGURE 4. Effects of glucose on NAD(P)H autofluorescence, $[Ca^{2+}]_i$ and (mt-)GRX1-roGFP2 fluorescence ratio in perifused human islets. A, effects of increasing glucose concentrations on NAD(P)H autofluorescence expressed as a percentage of the average fluorescence level during initial perifusion with G0.5. B, effects of glucose on fura-2 LR fluorescence ratio as an indicator of $[Ca^{2+}]_i$. C, effects of glucose on normalized mt-GRX1-roGFP2 fluorescence ratio. Results are means ± SE for 7-15 islets from two donors. A, B * $P<0.001$ *vs.* G0.5 and # $P<0.001$ for the effect of azide or high potassium. C, * $P<0.001$ *vs.* G0. The corresponding probe oxidation ratios (OxD) and glutathione redox potentials (E_{GSH}) are shown in table 2.

THIS IS NOT THE VERSION OF RECORD - see doi:10.1042/BJ20131361

Accepted Manuscript

Licenced copy. Copying is not permitted, except with prior permission and as allowed by law.
© 2014 The Authors Journal compilation © 2014 Biochemical Society

Biochemical Journal Immediate Publication. Published on 28 Mar 2014 as manuscript BJ20131361

FIGURE 5. A low H_2O_2 concentration unmasks the effects of glucose on GRX1-roGFP2 fluorescence ratio. Islet cell clusters expressing GRX1-roGFP2 were perifused with a Krebs solution containing 15 µM H_2O_2 and either 10, 0 or 30 mM glucose (Gn) before final application of 10 mM DTT then 1 mM H_2O_2 in the presence of G10 for normalization of the traces. Results are means ± SE for 3 experiments. * P<0.001 for the effect of H_2O_2 in G10; # P<0.01 for the effect of changes in glucose in the presence of H_2O_2.

FIGURE 6. Effects of cellular alkalinization and acidification on mt-GRX1-roGFP2 fluorescence ratio. Islets cell clusters expressing mt-GRX1-roGFP2 were perifused with a medium containing 10 mM glucose followed by application of 30 mM NH_4Cl to alkalinize the mitochondrial matrix, then 30 mM Na^+ acetate to acidify the compartment, before final application of 10 mM DTT then 1 mM H_2O_2 for normalization of the traces. Results are means ± SEM for 3 experiments. * P<0.05 for the transient effect of NH_4Cl and Na^+ acetate *vs.* end of previous condition.

FIGURE 7. Role of Ca^{2+} influx in glucose-induced changes in mt-GRX1-roGFP2 fluorescence ratio. Islet cell clusters loaded for 2h with fura-2 LR-acetoxymethylester (A, B) or expressing mt-GRX1-roGFP2 (C, D) were perifused with a Krebs solution containing various glucose concentrations and 500 µM tolbutamide (Tolbu, panelS A, C), 250 µM diazoxide (Dz, panels B, D) or 30 mM extracellular K^+ in the continued presence of diazoxide (B, D). Results are expressed as means ± SE for 3 experiments. * P<0.05 and ** P<0.001 *vs.* the previous condition. The corresponding probe oxidation ratios (OxD) and glutathione redox potentials (E_{GSH}) are shown in table 3.

FIGURE 8. Effects of superoxide dismutase 2 and mitochondrial catalase overexpression on mt-GRX1-roGFP2 fluorescence ratio. A, islet cell clusters expressing mt-GRX1-roGFP2 were infected with adenoviruses coding superoxide dismutase 2 (Ad-SOD2) and mitochondrial catalase (Ad-mCAT) (25 MOI each). They were then perifused with a Krebs solution containing G10 with increasing concentrations of H_2O_2 (A) or menadione (B), or various glucose concentrations (C). Islet cell clusters infected with Ad-Null (50MOI) were used as controls. Because the effect of H_2O_2 was reduced by mCAT overexpression, the data were normalized to the difference between the mean ratio measured from 4 min after addition of 10 mM DTT (set to 0%) and that measured from 4 min after addition of 100 µM aldrithiol (2,2'-dipyridyldisulfide, AT-2) (set at 100%) at the end of the experiments. Results are means ± SE for 3 experiments. A, B, * P<0.05 and ** P<0.001 for the effect of H_2O_2 or menadione in G10; # P<0.001 *vs.* Ad-Null-infected cell clusters. C, * P<0.01 *vs.* previous condition.

FIGURE 9. Effects of mitochondrial poisons on mt-GRX1-roGFP2 fluorescence ratio and NAD(P)H autofluorescence. Islet cell clusters expressing mt-GRX1-roGFP2 were perifused with a Krebs solution containing G10 then G2 (A, B) or G30 (D, E) and later exposed to 20 µM rotenone (A, D) or 5 mM azide (B, E) before final application of 10 mM DTT and 1 mM H_2O_2 for normalization of the traces. C and F, NAD(P)H autofluorescence was recorded in islets cell clusters stimulated from G0.5 to G2 or G30 before addition of 5 mM azide then 20 µM rotenone. Data are expressed as a percentage of the average fluorescence level during initial perifusion with G0.5. Results are means ± SE for 3 experiments. * P<0.05 and ** P<0.01 for the effect of glucose. # P<0.05 and ## P<0.01 for the effect of mitochondrial poisons.

THIS IS NOT THE VERSION OF RECORD - see doi:10.1042/BJ20131361

Accepted Manuscript

Licenced copy. Copying is not permitted, except with prior permission and as allowed by law.
© 2014 The Authors Journal compilation © 2014 Biochemical Society

Biochemical Journal Immediate Publication. Published on 28 Mar 2014 as manuscript BJ20131361

FIGURE 10. Effects of mitochondrial uncoupling on mt-GRX1-roGFP2 fluorescence ratio and NAD(P)H autofluorescence. Islet cell clusters expressing mt-GRX1-roGFP2 were perifused with a Krebs solution containing G10 then G2 (A) or G30 (C) and later exposed to 1 µM carbonyl cyanide p-trifluoromethoxyphenylhydrazone (FCCP) before final application of 10 mM DTT and 1 mM H_2O_2 for normalization of the traces. B, D, NAD(P)H autofluorescence was recorded in islets cell clusters stimulated from G0.5 to G2 or G30 before addition of 1 µM FCCP. Data are expressed as a percentage of the average fluorescence level measured during initial perifusion with G0.5. Results are means ± SE for 3 experiments. * $P<0.05$ and ** $P<0.01$ for the effect of glucose. # $P<0.001$ for the effect of FCCP.

FIGURE 11. Correlation between mt-GRX1-roGFP2 fluorescence ratio and NAD(P)H autofluorescence. Relationship between mt-GRX1-roGFP2 fluorescence ratio and NAD(P)H autofluorescence data recorded in islet cell clusters perifused under the experimental conditions depicted in figures 3 (glucose only), 7 (glucose + azide or rotenone) and 8 (glucose + FCCP). The data were fitted to a one phase exponential decay equation using GraphPad Prism 6.02 (r^2= 0.96).

THIS IS NOT THE VERSION OF RECORD - see doi:10.1042/BJ20131361

Accepted Manuscript

Licenced copy. Copying is not permitted, except with prior permission and as allowed by law.
© 2014 The Authors Journal compilation © 2014 Biochemical Society

Biochemical Journal Immediate Publication. Published on 28 Mar 2014 as manuscript BJ20131361

Figure 1

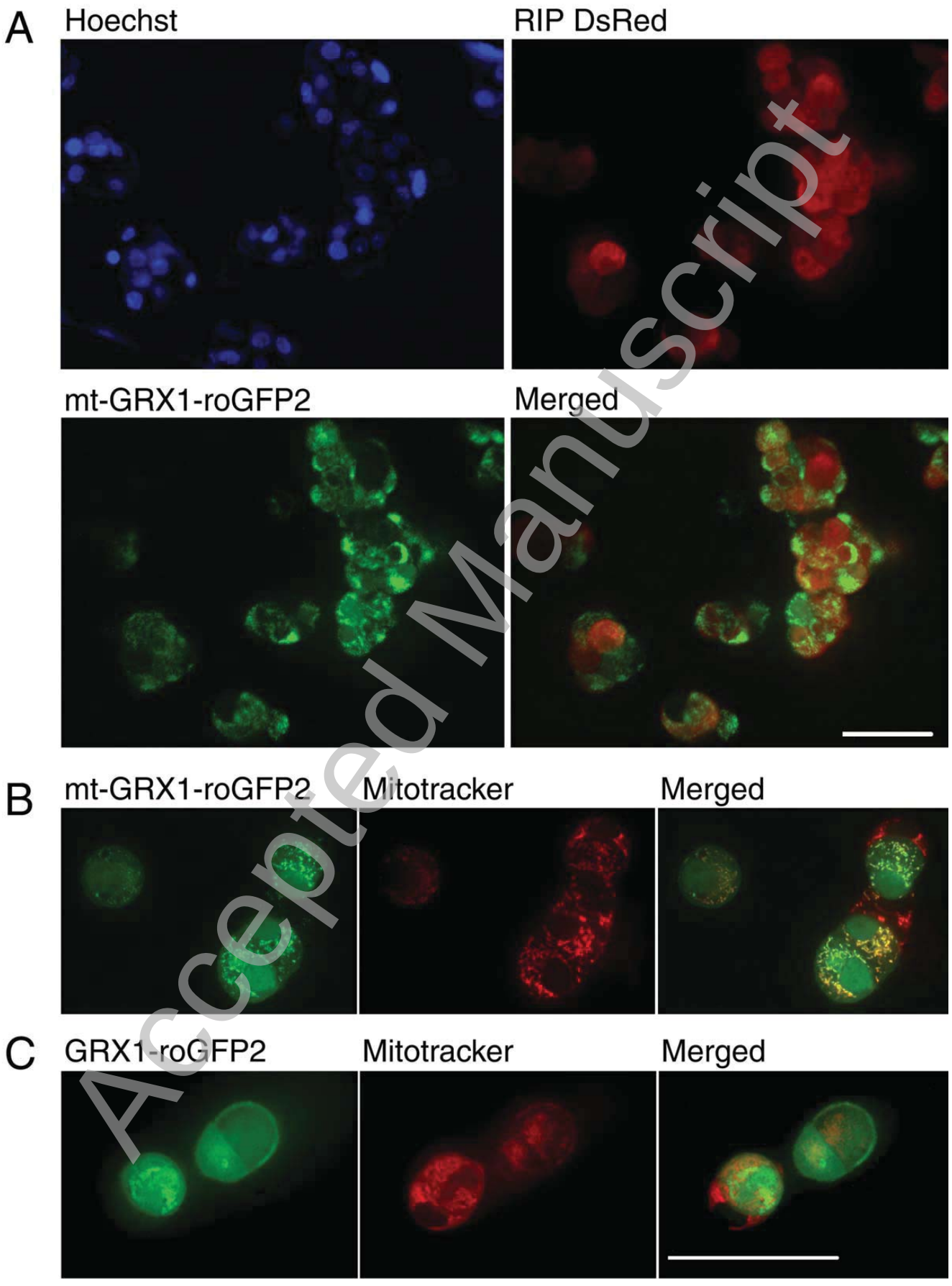

THIS IS NOT THE VERSION OF RECORD - see doi:10.1042/BJ20131361

Accepted Manuscript

Licenced copy. Copying is not permitted, except with prior permission and as allowed by law.
© 2014 The Authors Journal compilation © 2014 Biochemical Society

Biochemical Journal Immediate Publication. Published on 28 Mar 2014 as manuscript BJ20131361

FIGURE 2

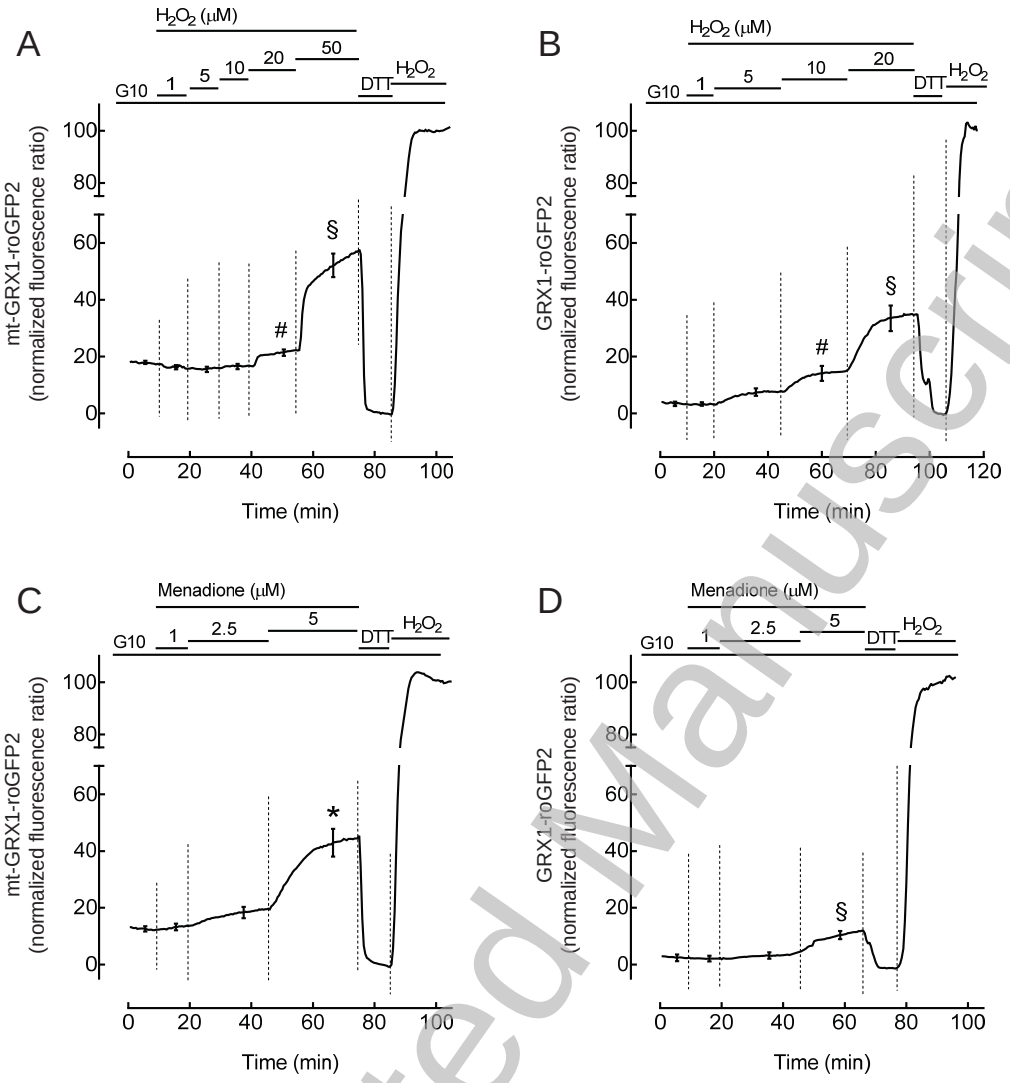

THIS IS NOT THE VERSION OF RECORD - see doi:10.1042/BJ20131361

Accepted Manuscript

Licenced copy. Copying is not permitted, except with prior permission and as allowed by law.
© 2014 The Authors Journal compilation © 2014 Biochemical Society

Biochemical Journal Immediate Publication. Published on 28 Mar 2014 as manuscript BJ20131361

FIGURE 3

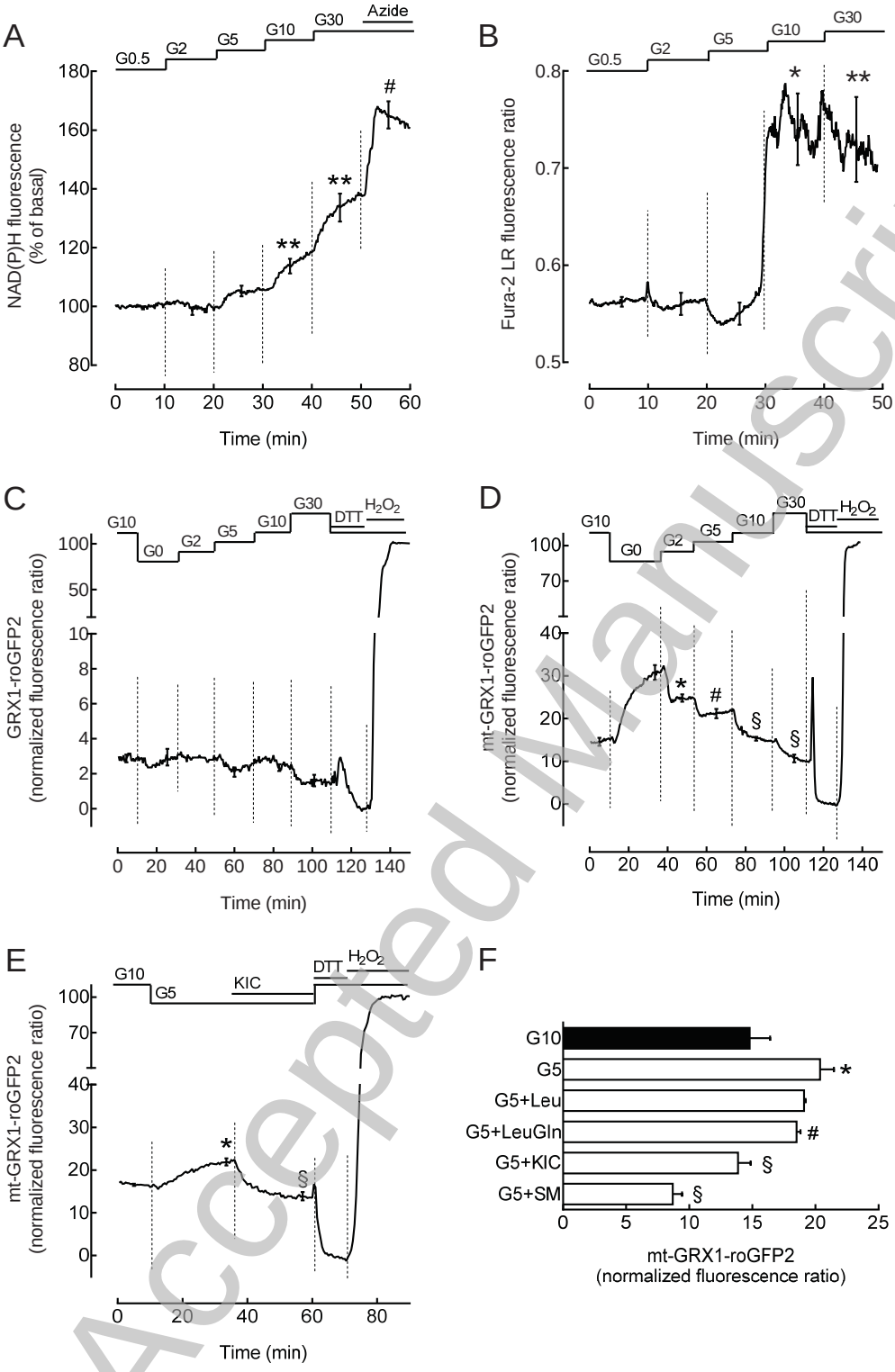

THIS IS NOT THE VERSION OF RECORD - see doi:10.1042/BJ20131361

Accepted Manuscript

Licenced copy. Copying is not permitted, except with prior permission and as allowed by law.
© 2014 The Authors Journal compilation © 2014 Biochemical Society

Biochemical Journal Immediate Publication. Published on 28 Mar 2014 as manuscript BJ20131361

FIGURE 4

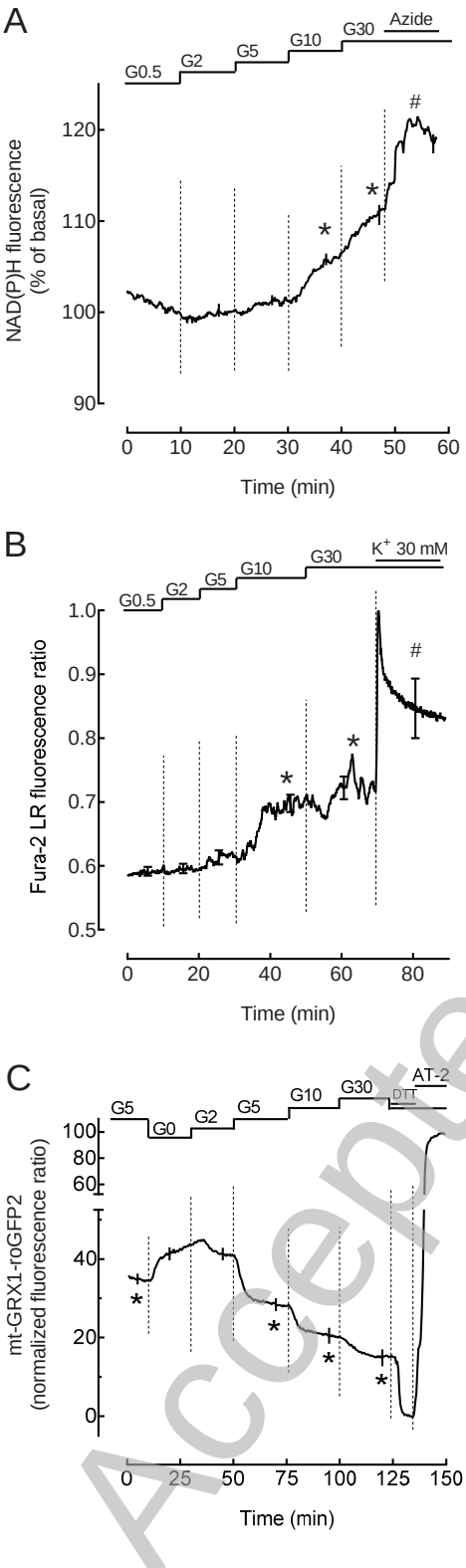

THIS IS NOT THE VERSION OF RECORD - see doi:10.1042/BJ20131361

Accepted Manuscript

Licenced copy. Copying is not permitted, except with prior permission and as allowed by law.
© 2014 The Authors Journal compilation © 2014 Biochemical Society

FIGURE 5

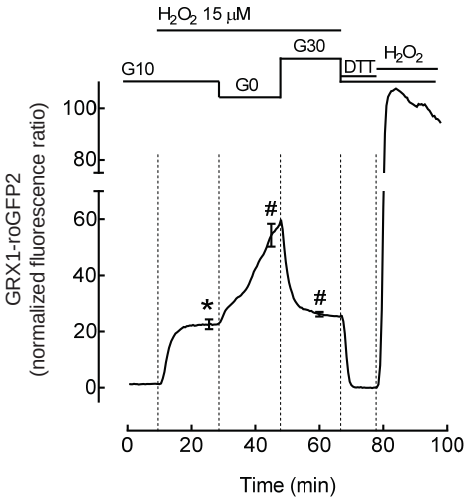

THIS IS NOT THE VERSION OF RECORD - see doi:10.1042/BJ20131361

Accepted Manuscript

Licenced copy. Copying is not permitted, except with prior permission and as allowed by law.
© 2014 The Authors Journal compilation © 2014 Biochemical Society

Biochemical Journal Immediate Publication. Published on 28 Mar 2014 as manuscript BJ20131361

FIGURE 6

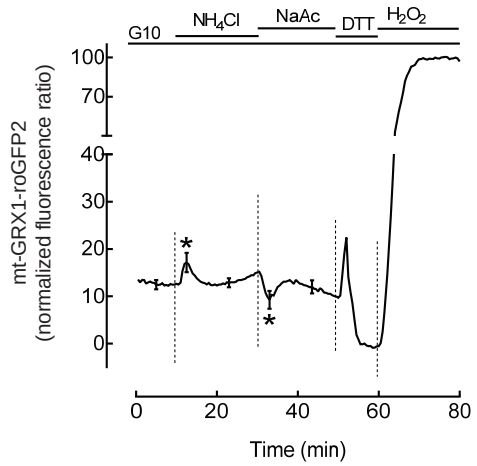

THIS IS NOT THE VERSION OF RECORD - see doi:10.1042/BJ20131361

Accepted Manuscript

Licenced copy. Copying is not permitted, except with prior permission and as allowed by law.
© 2014 The Authors Journal compilation © 2014 Biochemical Society

Biochemical Journal Immediate Publication. Published on 28 Mar 2014 as manuscript BJ20131361

FIGURE 7

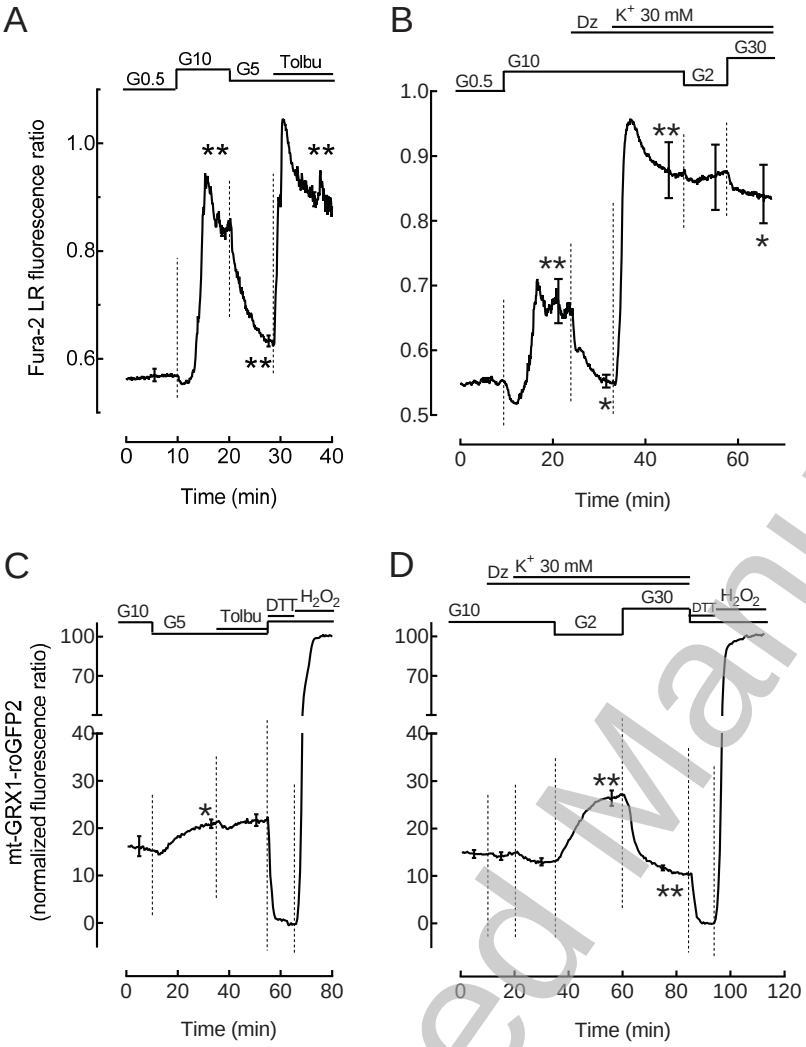

THIS IS NOT THE VERSION OF RECORD - see doi:10.1042/BJ20131361

Accepted Manuscript

Licenced copy. Copying is not permitted, except with prior permission and as allowed by law.
© 2014 The Authors Journal compilation © 2014 Biochemical Society

Biochemical Journal Immediate Publication. Published on 28 Mar 2014 as manuscript BJ20131361

FIGURE 8

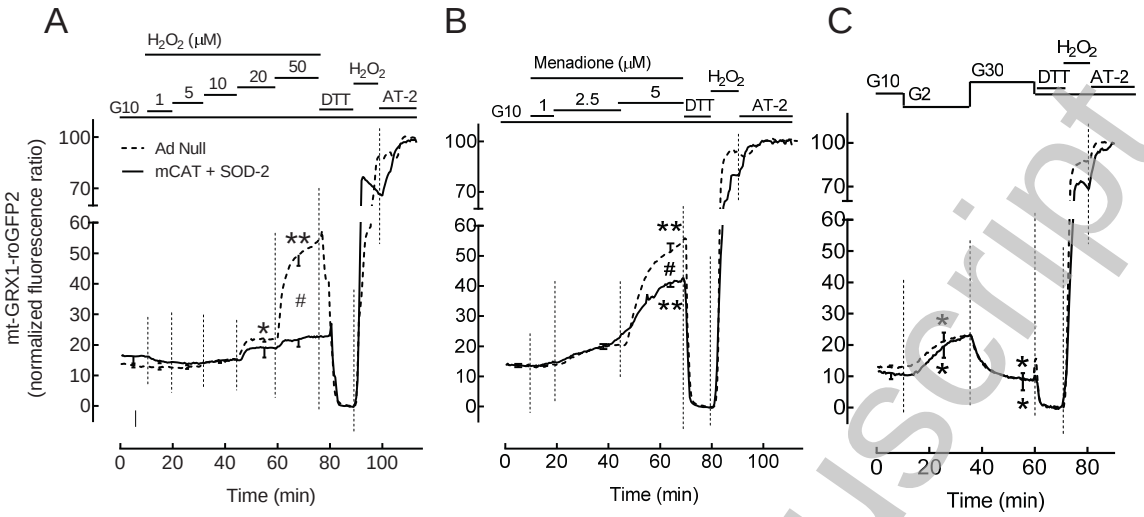

THIS IS NOT THE VERSION OF RECORD - see doi:10.1042/BJ20131361

Accepted Manuscript

Licenced copy. Copying is not permitted, except with prior permission and as allowed by law.
© 2014 The Authors Journal compilation © 2014 Biochemical Society

Biochemical Journal Immediate Publication. Published on 28 Mar 2014 as manuscript BJ20131361

FIGURE 9

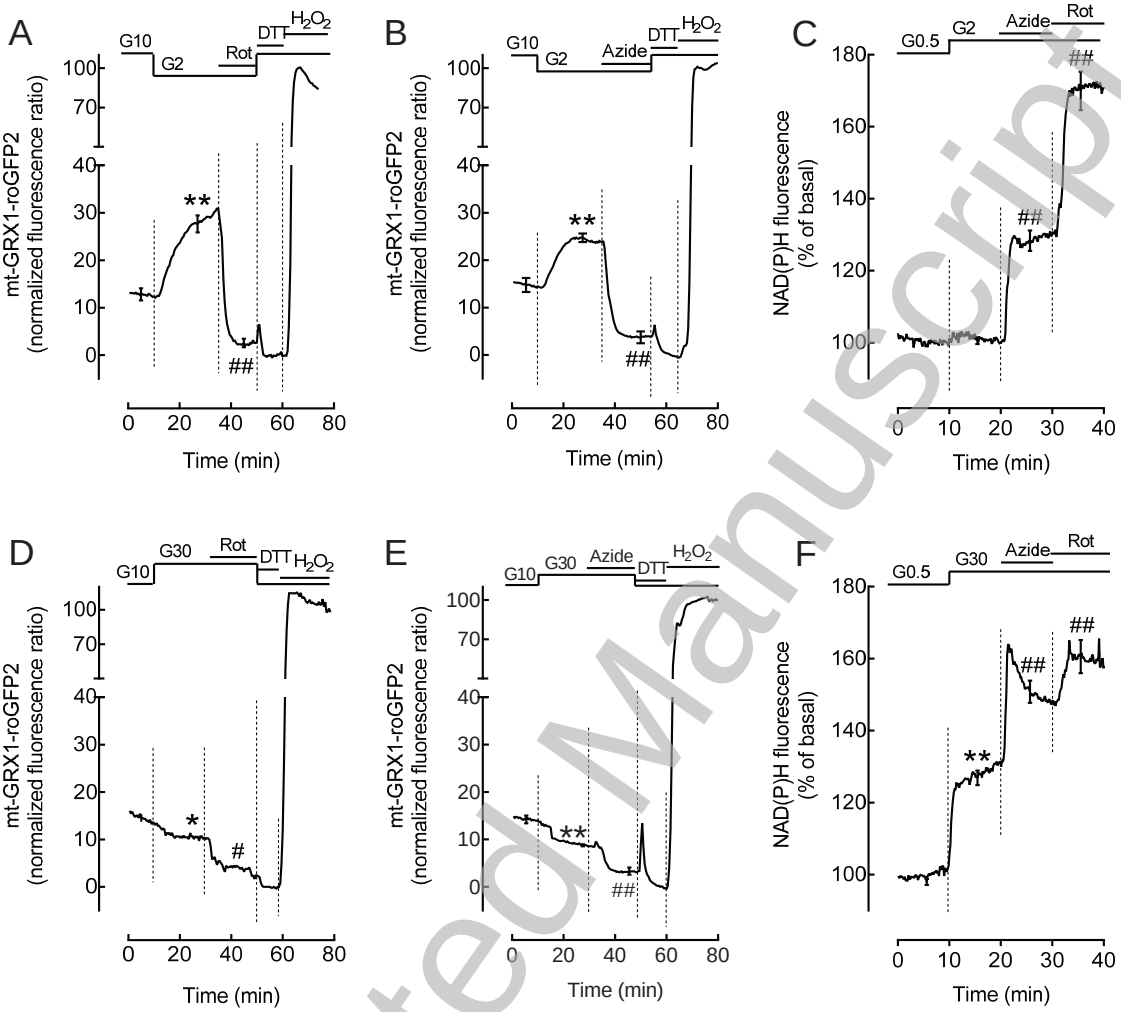

THIS IS NOT THE VERSION OF RECORD - see doi:10.1042/BJ20131361

Accepted Manuscript

Licenced copy. Copying is not permitted, except with prior permission and as allowed by law.
© 2014 The Authors Journal compilation © 2014 Biochemical Society

Biochemical Journal Immediate Publication. Published on 28 Mar 2014 as manuscript BJ20131361

FIGURE 10

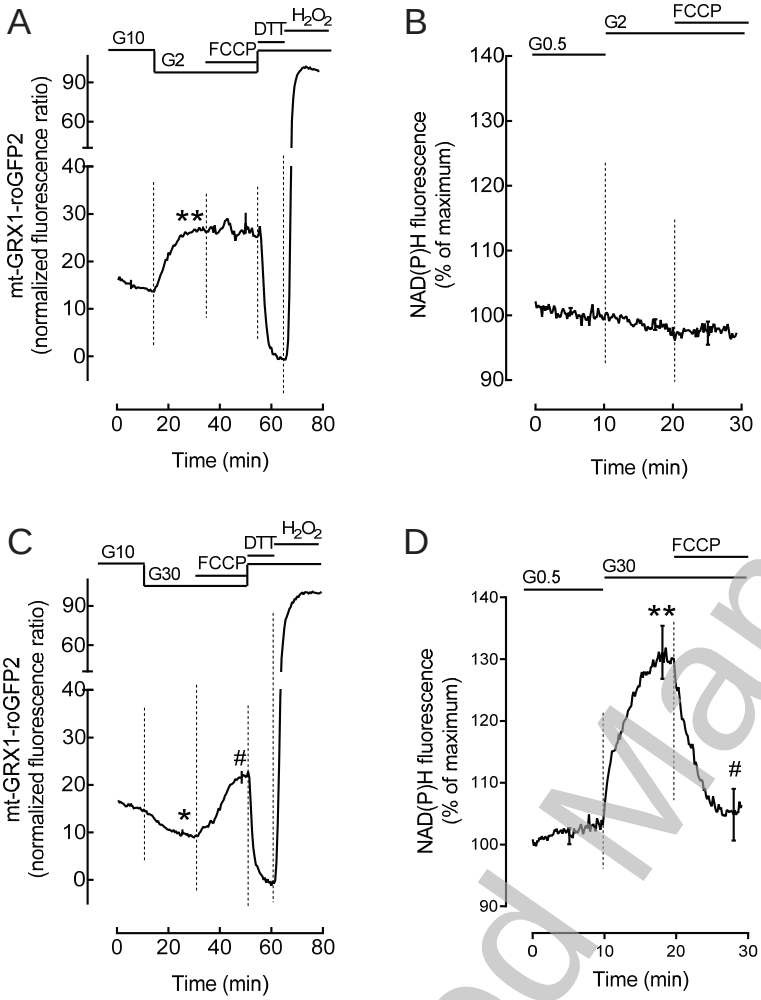

THIS IS NOT THE VERSION OF RECORD - see doi:10.1042/BJ20131361

Accepted Manuscript

Licenced copy. Copying is not permitted, except with prior permission and as allowed by law.
© 2014 The Authors Journal compilation © 2014 Biochemical Society

Biochemical Journal Immediate Publication. Published on 28 Mar 2014 as manuscript BJ20131361

FIGURE 11

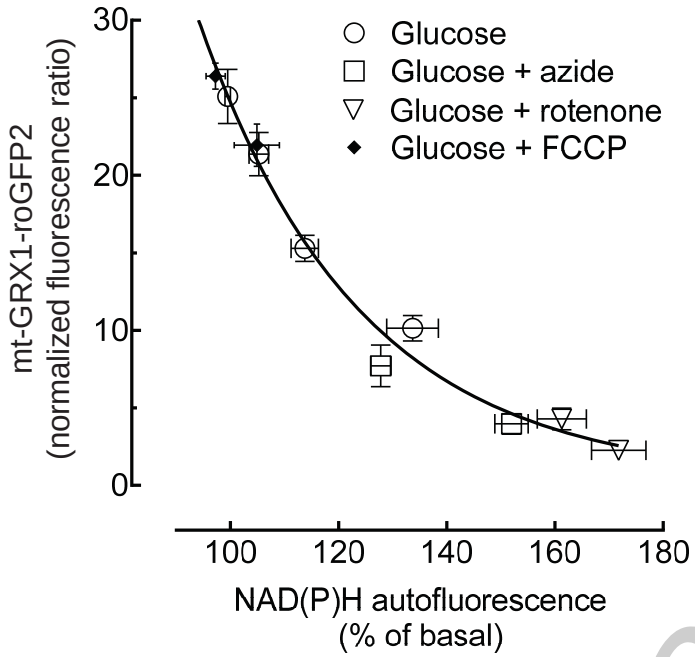

THIS IS NOT THE VERSION OF RECORD - see doi:10.1042/BJ20131361

Accepted Manuscript

Licenced copy. Copying is not permitted, except with prior permission and as allowed by law.
© 2014 The Authors Journal compilation © 2014 Biochemical Society